Proceedings of the Combustion Institute SAND2020-1223C

Multi-Injection Effects on the Structure of Edge Flames at Diesel Conditions

--Manuscript Draft--

Manuscript Number:	PROCI-D-19-00072
Article Type:	4. Laminar Flames
Keywords:	Polybrachial; Multi Injection; Chemical Explosive Mode Analysis; N-dodecane; Polybrachial Flame
Corresponding Author:	Martin Rieth Sandia National Laboratories UNITED STATES
First Author:	Martin Rieth
Order of Authors:	Martin Rieth
	Marc Day
	Kweon Chol-Bum
	Jacob Temme
	Tianfeng Lu
	Jacqueline Chen
Abstract:	Compression ignition engines are widely utilized in unmanned aerial vehicle (UAV) and heavy-duty transportation sectors. For these engines, low-temperature multi-injection strategies are known to improve operation in terms of pollutant emission, noise and controllability. However, a fundamental understanding of the interaction of multiple injections is still missing. We investigate the effect of multiple injections of n-dodecane under diesel engine conditions on lifted flame stabilization for a canonical configuration corresponding to a two-dimensional partially premixed laminar flame. The configuration is motivated by the experiments performed by Skeen et al. (SAE International Journal of Engines, 2015) which showed the effect of the pilot injection on accelerating the ignition of the main injection through mixing of equilibrium products of combustion or low-temperature cool flame intermediate species generated from high and low-temperature ignition of the pilot, respectively, with the environment depending on the ambient temperature. In the present study temperatures representative of intermediate and low-temperature ambient conditions were selected to assess their effect on the local lifted flame structure and propagation characteristics.

Multi-Injection Effects on the Structure of Edge Flames at Diesel Conditions

Martin Rieth[a,*], Marc Day[b], Chol-Bum Kweon[c], Jacob Temme[c], Tianfeng Lu[d], Jacqueline Chen[a]

[a] *Combustion Research Facility, Sandia National Laboratories, Livermore, California, USA*
[b] *Lawrence Berkeley National Laboratory, Berkeley, California, USA*
[c] *S Army Research Laboratory, Aberdeen Proving Ground, Maryland, USA*
[d] *University of Connecticut, Storrs, Connecticut, USA*

Abstract

Compression ignition engines are widely utilized in unmanned aerial vehicle (UAV) and heavy-duty transportation sectors. For these engines, low-temperature multi-injection strategies are known to improve operation in terms of pollutant emission, noise and controllability. However, a fundamental understanding of the interaction of multiple injections is still missing. We investigate the effect of multiple injections of n-dodecane under diesel engine conditions on lifted flame stabilization for a canonical configuration corresponding to a two-dimensional partially premixed laminar flame. The configuration is motivated by the experiments performed by Skeen et al. (SAE International Journal of Engines, 2015) which showed the effect of the pilot injection on accelerating the ignition of the main injection through mixing of equilibrium products of combustion or low-temperature cool flame intermediate species generated from high and low-temperature ignition of the

*Corresponding author: Martin Rieth, mrieth@sandia.gov
Email address: mrieth@sandia.gov (Martin Rieth)

pilot, respectively, with the environment depending on the ambient temperature. In the present study temperatures representative of intermediate and low-temperature ambient conditions were selected to assess their effect on the local lifted flame structure and propagation characteristics.
Keywords:
Polybrachial, Multi Injection, Chemical Explosive Mode Analysis,
N-dodecane, Polybrachial Flame

1. Introduction

Multi-injection strategies are known to improve compression ignition engine operation in terms of, e.g., pollutant emission, noise and controllability [1, 2]. While this has been shown experimentally, a fundamental understanding of the ignition process under multi-injection conditions is still missing.

Skeen et al. [3] carried out detailed n-dodecane multi-injection experiments in the well-characterized Sandia Spray A vessel under a range of conditions. Depending on the ambient conditions, different ignition behaviors were observed. At higher temperatures (i.e, 900 K), the first injection ignited prior to the start of the second injection, leading to advanced ignition of the second injection due to mixing with hot products from the first injection. At lower temperatures (i.e., 750 K), the first injection did not ignite prior to mixing with the first injection, but rather provided low-temperature combustion species that accelerate the ignition of the second injection such that first and second injections ignite only after mixing with each other. In general, the ignition of the second injection can be affected by enthalpy effects (i.e., an increased temperature from the ignition of the first injection) or by chem-

ical effects (i.e., the interaction of low-temperature and/or high-temperature radicals from the first injection and the fresh fuel from the second injection), or both, depending on the conditions. The extent to which products, radicals or heat are present is additionally controlled by the dwell time between the two injections, leaving the first injection more or less time to react prior to mixing with the second injection. Temme et al. [4] studied the effect of injection pressure on multi-injection ignition of JP-8 fuel, and found an ignition delay increase at higher fuel injection pressure for the double injections due to leaner mixtures. The effect of dwell time has been studied by Cung et al., who compared Reynolds-averaged Navier-Stokes (RANS) simulations to multi-injection experiments with a variation of the dwell time between the injections. Depending on the dwell time, the second injection mixes with a burning flame, hot products or cooler diluted products. Recent numerical work, based on RANS [5] and large eddy simulations (LES) [1, 6] shed some additional light on the ignition process of the second injection. These LES give a good indication of the global spray evaporation and combustion behavior, but cannot give a full account of the complex interaction of transport and chemistry due to the need for modeling.

We intend to elucidate some of the chemical and transport effects that affect ignition and combustion at low temperature multi-injection compression ignition conditions. To give a first account of these details, we chose a simplified configuration of a two-dimensional partially premixed laminar flame that has recently been used to investigate fundamental flame properties of complex fuels relevant for transportation applications. Krisman et al. [7] showed the effect of temperature on the flame structure and stabi-

lization mechanism for dimethyl ether (DME) at 40 atmospheres. At low temperature, they reported a tribrachial flame stabilized by conduction and diffusion-assisted flame propagation. With increasing temperatures, additional branches occurred and the flames were increasingly stabilized by auto-ignition, as evidenced by transport budgets of key species. Deng et al. [8, 9] studied the effect of inlet velocity on a DME flame and made similar observations as changes in inlet velocity lead to changes in residence time ahead of the flame front affecting the competition of auto-ignition and flame propagation. In addition, they employed the Chemical Explosive Mode Analysis (CEMA) [10] to elucidate the controlling reaction steps. Dalakoti et al. [11] studied two-dimensional partially premixed laminar n-dodecane flames in the context of the ECN Spray A [12]. In addition to inflow velocity, they studied the effect of scalar dissipation rate on the flame structure and stabilization mechanism, and suggested a characteristic triple flame propagation velocity into low-temperature combustion products as the velocity at which the triple point showed maximum sensitivity to the inlet velocity.

In a multi-injection setting, the environment is effectively changed from a pure oxidizer to a mixture of partially reacted fuel and oxidizer (the extent to which the mixture is reacted depending on temperature, dwell time, etc.) for the second injection. Depending on the conditions, the second injection typically first mixes with a lean partially reacted mixture. Figure 1 shows Direct Numerical Simulations (DNS) of downscaled versions of the experiment by Skeen et al. [3] at 750 K and 900 K, 60 atm and with injection durations of 0.5 ms separated by a dwell time of 0.5 ms that will be reported in detail elsewhere. However, we based the parameter study presented here on the

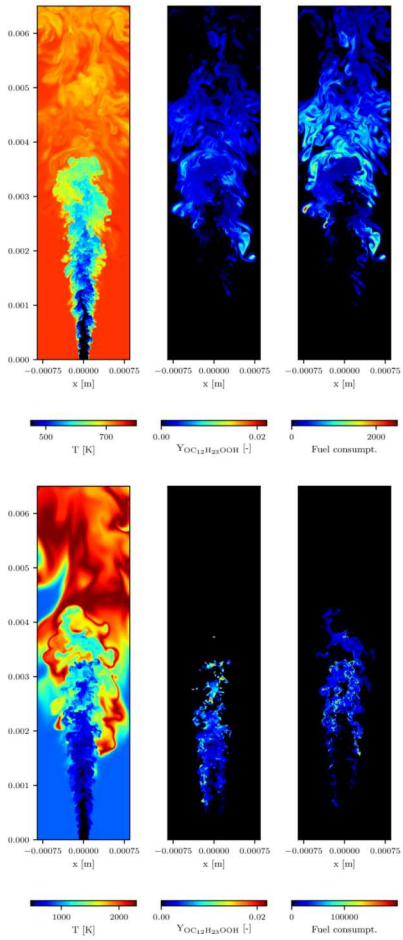

Figure 1: Instantaneous snapshots from a cut through 3D multi-injection DNS at 750K (upper row) and 900K (lower row) and 60 atm at approximately 1.37ms after start of the first injection and 0.37ms after start of the second injection showing temperature, ketohydroperoxide radical mass fraction and fuel consumption rate (from left to right). The images do not include the full extent of the computational domain.

DNS and the experiment. With a first injection setting of 0.5 ms and a dwell time of 1 ms, the fluid age difference between fluid from the first and second injection is largely between 0.5 and 1 ms. At 750 K, ignition of the first

injection does not occur before the second injection interacts with the first injection. However, the fist injection provides low-temperature species that accelerate the ignition. At 900 K conditions, the second injection occurs in the presence of hot products from the first injection that has already ignited at the time of the start of the second injection.

We approximate the conditions the second injection encounters in our idealized 2D simulations by changing the composition of the oxidizer side of the partially premixed flames. In addition to a case that considers pure oxidizer (corresponding to a single injection), we add a small amount of fuel to the oxidizer and let it react in a separate zero-dimensional ignition calculation for a specified duration. We then prescribe the partially reacted mixture at that specified time as the boundary condition for the oxidizer stream. We considred an additional case with the oxidizer with fuel at equilibrium conditions for the 900 K case to reflect that a fully burning flame is established by the time the second injection mixes with the fist injection.

This allows us to investigate the chemical and laminar transport effects responsible for advancing the ignition of the second injection in an isolated fashion, i.e., without the additional complexity of turbulence-flame interaction present in technical devices or in aforementioned DNS. Ultimately, the results presented here will provide a reference to help understand the turbulent cases.

2. Numerical Configuration

The partially premixed flames are established in a two-dimensional domain of 4.096 mm $\times$ 2.048 mm in the transverse (x) and streamwise (y)

directions, respectively. A uniform inlet velocity is prescribed at the inlet of the domain (at y=0 mm). Species and enthalpy profiles at the inlet are prescribed based on a smooth tanh profile with a thickness of 0.1 mm. The oxidizer has a composition of 15% oxygen and 85% nitrogen by volume in accordance to the experiments [3]. Based on related work by Dalakoti et al. [11], a mixture fraction of Z=0.45 is imposed on the fuel side, which is representative of the conditions at the location where the liquid n-dodecane jet in the experiment is evaporated. We employ a reduced n-dodecane mechanism with 35 species [13] that has been reduced from a skeletal mechanism targeted at engine calculations including both high- and low-temperature oxidation pathways [14].

We consider several cases corresponding to different dwell times or, more generally, different times between the interaction of first and second injections. We choose a representative mixture fraction of $Z_{ox} = 0.01$ in the oxidizer stream for the cases representing multi-injection. The different dwell times are represented by different times the lean fuel-oxidizer mixture reacts in a separate zero-dimensional constant volume ignition calculation. The partially reacted mixture from the zero-dimensional calculation is then used as the boundary condition for the oxidizer stream. Table 2 summarizes the different cases including temperature and major species present in the oxidizer stream of the multi-injection cases.

All results are obtained with the adaptive mesh refinement low-Mach reacting flow solver PeleLM, which is based on a projection-based algorithm presented by Day & Bell [15]. A base grid of 512×256 cells and three levels of refinement are used in the region around the flame, leading to the finest-level

resolution of 1 μm, sufficient to resolve the thinnest flame features.

Case	Temperature	Major species mass fractions in the oxidizer stream
		750 K cases
Standard	750K	O_2: 0.168
0.1 ms	738.97K	O_2: 0.167, $NC_{12}H_{26}$: 0.01, $OC_{12}H_{23}OOH$: $1.15 \cdot 10^{-8}$
0.5 ms	739.68K	O_2: 0.166, $NC_{12}H_{26}$: 0.097, $OC_{12}H_{23}OOH$: $3.44 \cdot 10^{-4}$, H_2O: $3.15 \cdot 10^{-5}$, $C_{12}H_{25}O_2$: 1
1.0 ms	754.74K	O_2: 0.164, $NC_{12}H_{26}$: 0.0054, $OC_{12}H_{23}OOH$: $4.30 \cdot 10^{-3}$, H_2O: $8.9 \cdot 10^{-4}$, CO: $7.2 \cdot 10^{-}$
		900 K cases
Standard	900 K	O_2: 0.168
0.1 ms	916.92 K	O_2: 0.161, $NC_{12}H_{26}$: 0.0048, CO: $3.2 \cdot 10^{-3}$, H_2O: $2.40 \cdot 10^{-3}$, $OC_{12}H_{23}OOH$: $2.12 \cdot 10$
0.5 ms	926.22 K	O_2: 0.160, $NC_{12}H_{26}$: 0.0040, CO: $4.3 \cdot 10^{-3}$, H_2O: $2.98 \cdot 10^{-3}$, CO_2: $1.5 \cdot 10^{-4}$
1.0 ms	938.46 K	O_2: 0.158, $NC_{12}H_{26}$: 0.0030, CO: $5.4 \cdot 10^{-3}$, H_2O: $3.7 \cdot 10^{-3}$, C_2H_4: $3.0 \cdot 10^{-3}$
Eq	1258.8 K	O_2: 0.13, CO_2: 0.031, H_2O: 0.0137

Table 1: Major species mass fractions excluding N2 in the oxidizer stream for the different cases considered in this study.

3. Results

Figures 2 and 3 present heat release isocontours for the 750 K and 900 K cases, respectively, with the oxidizer stream being pure oxidizer and a fuel/oxidizer mixture with Z=0.01 that has reacted for 0.1, 0.5 and 1 ms. The inlet velocity is set to 0.5 m/s for the 750 K and 2 m/s for the 900 K case. The flame structure for the 750 K and 900 K cases is different, with a discernible upstream low-temperature heat release branch forming in the 900 K case, consistent with earlier studies at similar temperatures (e.g., DME at 700 & 900 K [7] and n-dodecane at 900 K [11]). Flames at 750 and 900 K show different sensitivity toward changes in oxidizer age/composition. However, the

flame location advances toward the inlet for all cases where partially reacted fuel is present in the oxidizer stream. A summary of the advancement of the flame position is given in Fig. 4, where the age of the fluid at the time of maximum heat release is shown. We obtain the age of the fluid by solving an additional transport equation, equivalent to, e.g. [16], with an initial time assigned at the inlet, irrespective of the age of the oxidizer. The ignition time is advanced significantly for the 750 K case, from approximately 1.6 ms to around 0.8ms with an oxidizer age of 0.5 ms. The reduction by 0.8ms is quite remarkable given that the oxidizer only had 0.5 ms to react prior to being injected into the simulation. The ignition time increases again at an oxidizer age of 1 ms, suggesting that under these conditions there is an 'optimal' dwell time with respect to ignition delay. This also implies that a time of 0.5 ms produces an optimal composition to advance the overall ignition when mixing with fresh fuel, analyzed in more detail below. At 900 K, different oxidizer times do not change the ignition times as strongly as at 750 K. However, a strong decrease in ignition delay time is observed for the case of equilibrium in the oxidizer stream. Table 2 summarizes temperature and the major species in the oxidizer stream for all cases. At 750 K and 0.1 ms oxidizer age, only a very small amount of keto-hydroperoxide ($OC_{12}H_{23}OOH$) is produced. At 0.5 ms, the mass fraction of $OC_{12}H_{23}OOH$ increases to $3.44 \cdot 10^{-4}$ and to $4.30 \cdot 10^{-3}$ at 1 ms. Other major species include products such as H_2O and CO, found at increasing mass fractions for larger oxidizer times. For the 900 K case, products are formed much more quickly and early low-temperature combustion species are only present with low mass fractions, mostly at an oxidizer time of 0.1 ms. The relevance of

individual species is investigated in the following.

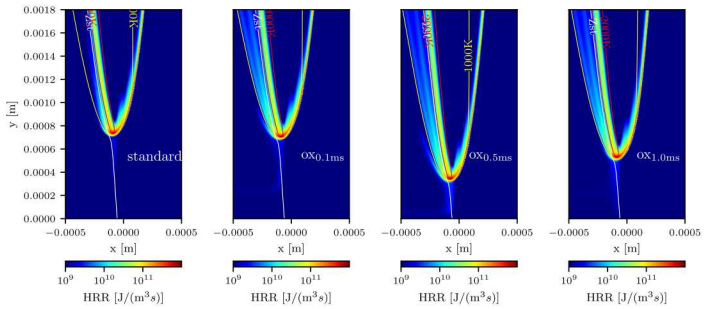

Figure 2: Heat release for the 750 K cases. Iso-lines show stoichiometric mixture fraction and 1000/2000 K.

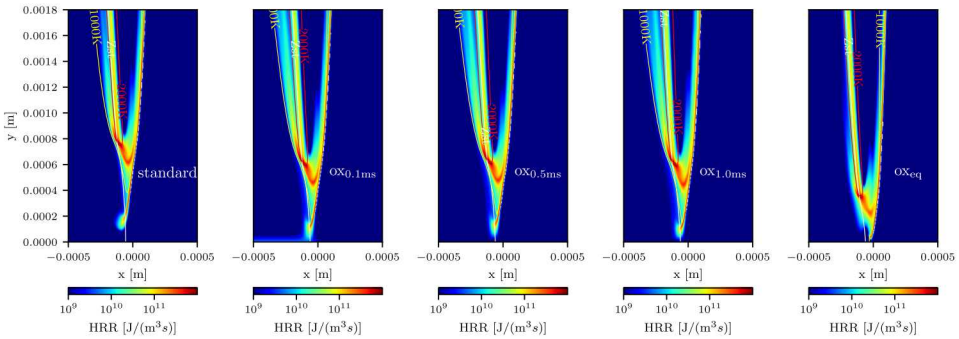

Figure 3: Heat release for 900 K case. Iso-lines show stoichiometric mixture fraction and 1000/2000 K.

To analyze the differences between the cases in detail, we sample conditions along the stoichiometric mixture fraction iso-line. In addition, we shift the coordinate in the flow direction (y) such that $y^*_{Z=Z_{\mathrm{st}}} = 0$ corresponds to the location at which T=1500 K (900 K case) or T=1000 K (750 K case) is

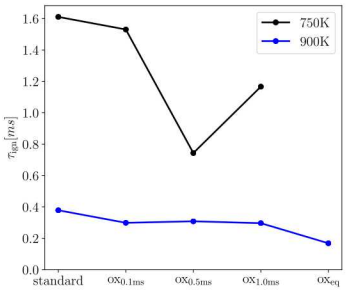

Figure 4: Ignition times from 750 K and 900 K from the 2D edge flame calculations.

exceeded. Figure 5 shows the temperature along the mixture fraction iso-line at stoichiometric conditions. Compared to the standard and 0.1 ms cases, 0.5 and 1 ms cases show an earlier and steeper increase in temperature ahead of the flame, which can be attributed to the chemical species present in the oxidizer stream since the initial temperature varies only slightly between the cases. The temperature increase is strongest for the 0.5 ms case, followed by the 1 ms case. This is further shown in Fig. 6, showing the heat release rate along the stoichiometric mixture fraction iso-line. All cases feature a peak corresponding to low-temperature ignition followed quickly by a second peak corresponding to high-temperature ignition. The peak heat release rates differ significantly between the different cases, e.g., the 0.5 ms and 1 ms cases shows a peak heat release rate increase by more than a factor of 3 and 2, respectively, compared to the standard case. At 900 K, Figs 8 and 10, the differences between the standard case and the 0.1, 0.5 and 1.0 ms cases is smaller. The delay between low- and high-temperature ignition decreases compared to the standard case to the same extent with 0.1, 0.5 and 1.0 ms oxidizer age, respectively. Peak heat release rates are similar for all cases, however, the equilibrium case does not show low-temperature ignition but

directly and rapidly transitions to high-temperature ignition.

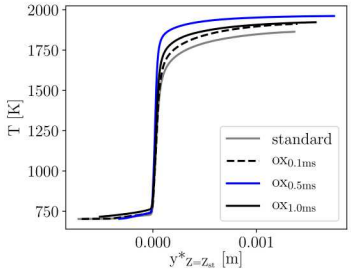

Figure 5: Temperature along Z_{st} for the 750 K cases, the spatial coordinate along the Z_{st} is shifted such that the location of 0 m corresponds to the location at which 1000 K are exceeded.

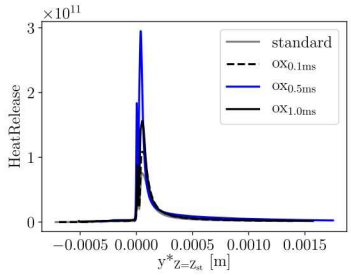

Figure 6: Heat release rate along Z_{st} for the 750 K cases, the spatial coordinate along the Z_{st} is shifted such that the location of 0 m corresponds to the location at which 1000 K are exceeded.

We utilize the Chemical Explosive Mode Analysis [10] to identify species and reactions responsible for the differences in ignition behavior between the different cases. We compute the species explosion indices along the stoichiometric mixture fraction iso-line, integrate their values from the domain inlet up to the point of ignition and then re-normalize them. This way we get the overall contribution of the different species up to the point of ignition. At

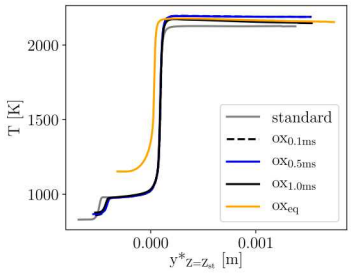

Figure 7: Temperature along Z_{st} for the 900 K cases, the spatial coordinate along the Z_{st} is shifted such that the location of 0 m corresponds to the location at which 1500 K are exceeded.

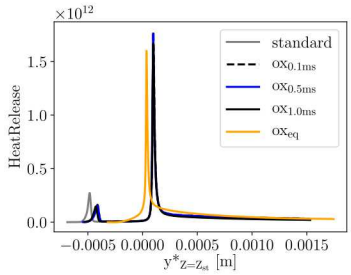

Figure 8: Heat release rate along Z_{st} for the 900 K cases, the spatial coordinate along the Z_{st} is shifted such that the location of 0 m corresponds to the location at which 1500 K are exceeded..

750 K, both keto-hydroperoxide and temperature show large contributions to the explosive mode, but this strongly shifts comparing the different oxidizer cases. For later oxidizer times, as the temperature increases, temperature becomes more important to drive ignition. The trend for keto-hydroperoxide is the opposite. Even though keto-hydroperoxide mass fractions in the oxidizer stream increase with oxidizer time, the importance for driving ignition decreases. At 0.5 ms oxidizer time there is a balance between the importance of temperature and keto-hydroperoxide leading to optimal conditions

with respect to early ignition. There are other species that contribute to ignition, but to a lesser extent. In general, species from early reaction steps (e.g., $OC_{12}H_{12}H_{24}OOH$) contribute more strongly for early oxidizer times, and vice versa for species that are formed at a later stage (e.g., H_2O_2).

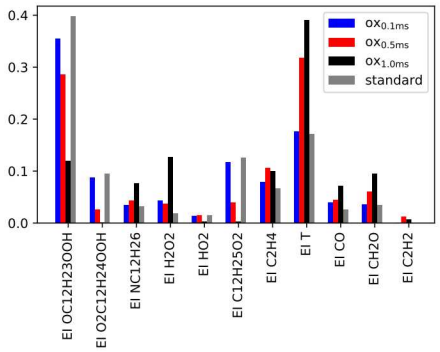

Figure 9: Comparison of explosion indices for the 750 K case.

The explosion indices at 900 K are distributed in a very different way compared to the 750 K case. Most notably, temperature is dominant for all cases. Compared to the 750 K case, the importance of keto-hydroperoxide has decreased significantly, but still contributes for all cases except the equilibrium case. At 900 K equilibrium conditions, the species dependence shifts to C_2H_4 and HO_2, albeit still showing small importance. The variability in the extent that different species contribute seems to be smaller for the 900 K case across the different oxidizer residence time conditions, with the exception of the equilibrium case.

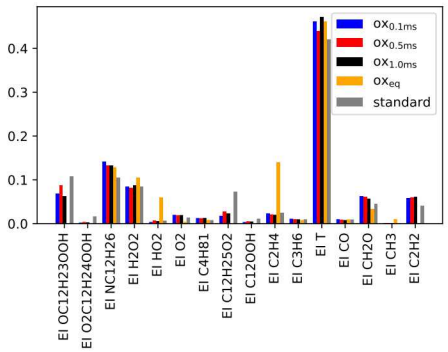

Figure 10: Comparison of explosion indices for the 900 K case.

4. Conclusions

Based on n-dodecane multi-injection experiments and DNS, we have conducted a study to better understand multi-injection ignition processes where the second injection mixes with hot products or intermediate species from the first injection, depending on the ambient and injection conditions. The study was done in a simplified two-dimensional laminar edge flame configuration, where the effect of the first injection is incorporated by adding fuel to the oxidizer stream and allowing the oxidizer with the added fuel to react for different amounts of time, and then prescribing this partially reacted mixture as a boundary condition for the laminar partially premixed simulations. The analysis showed that the low-temperature case at 750 K is very sensitive to the oxidizer 'cooking' time, even though the oxidizer stream does not produce significantly elevated temperatures. Based on CEMA results, we found a strong sensitivity toward keto-hydroperoxide as well as to temperature. At 900 K, the sensitivity to the oxidizer time is smaller. In general, the ignition of the higher temperature case at 900 K is more strongly driven by tempera-

ture than by a single dominant species such as in the 750 K case. The results suggest that at a desired low-temperature operation, dwell time may have a much stronger impact on the ignition delay. The results also imply that there could be kinetically optimal dwell time settings under certain conditions with respect to the first injection accelerating the ignition of the second injection. However, this has to be confirmed by testing different chemical mechanisms and fuels.

Acknowledgments

Support for the Sandia authors was provided by the U.S. Department of Energy, Office of Vehicle Technologies and by the U.S. Army Research Laboratory. Sandia National Laboratories is a multimission laboratory managed and operated by National Technology and Engineering Solutions of Sandia, LLC., a wholly owned subsidiary of Honeywell International, Inc., for the U.S. Department of Energy's National Nuclear Security Administration under contract DE-NA-0003525. We thank Lyle Pickett for helpful discussions.

References

[1] A. A. Moiz, M. M. Ameen, S.-Y. Lee, S. Som, Study of soot production for double injections of n-dodecane in CI engine-like conditions, Combustion and Flame 173 (2016) 123–131.

[2] J. O'Connor, M. Musculus, Post injections for soot reduction in diesel engines: a review of current understanding, SAE International Journal of Engines 6 (2013) 400–421.

[3] S. Skeen, J. Manin, L. M. Pickett, Visualization of ignition processes in high-pressure sprays with multiple injections of n-dodecane, SAE International Journal of Engines 8 (2015) 696–715.

[4] J. Temme, V. Coburn, C.-B. Kweon, Kilohertz mie scattering and oh* chemiluminescence imaging of jp-8 multiple injections using a 250 mpa fuel injector, in: SAE Technical Paper, SAE International, 2017. doi:10.4271/2017-01-0832.

[5] M. Bolla, M. A. Chishty, E. R. Hawkes, S. Kook, Modeling combustion under engine combustion network Spray A conditions with multiple injections using the transported probability density function method, International Journal of Engine Research 18 (2017) 6–14.

[6] A. Hadadpour, M. Jangi, K. M. Pang, X. Song Bai, The role of a split injection strategy in the mixture formation and combustion of diesel spray: A large-eddy simulation, Proceedings of the Combustion Institute 37 (2019) 4709–4716.

[7] A. Krisman, E. R. Hawkes, M. Talei, A. Bhagatwala, J. H. Chen, Polybrachial structures in dimethyl ether edge-flames at negative temperature coefficient conditions, Proceedings of the Combustion Institute 35 (2015) 999 – 1006.

[8] S. Deng, P. Zhao, M. E. Mueller, C. K. Law, Autoignition-affected stabilization of laminar nonpremixed dme/air coflow flames, Combustion and Flame 162 (2015) 3437 – 3445.

[9] S. Deng, P. Zhao, M. E. Mueller, C. K. Law, Stabilization of laminar nonpremixed dme/air coflow flames at elevated temperatures and pressures, Combustion and Flame 162 (2015) 4471 – 4478.

[10] T. F. LU, C. S. YOO, J. H. CHEN, C. K. LAW, Three-dimensional direct numerical simulation of a turbulent lifted hydrogen jet flame in heated coflow: a chemical explosive mode analysis, Journal of Fluid Mechanics 652 (2010) 45–64.

[11] D. K. Dalakoti, A. Krisman, B. Savard, A. Wehrfritz, H. Wang, M. S. Day, J. B. Bell, E. R. Hawkes, Structure and propagation of two-dimensional, partially premixed, laminar flames in diesel engine conditions, Proceedings of the Combustion Institute 37 (2019) 1961 – 1969.

[12] L. M. Pickett, C. L. Genzale, G. Bruneaux, L.-M. Malbec, L. Hermant, C. Christiansen, J. Schramm, Comparison of diesel spray combustion in different high-temperature, high-pressure facilities, SAE International Journal of Engines 3 (2010) 156–181.

[13] G. Borghesi, A. Krisman, T. Lu, J. H. Chen, Direct numerical simulation of a temporally evolving air/n-dodecane jet at low-temperature diesel-relevant conditions, Combustion and Flame 195 (2018) 183–202.

[14] T. Yao, Y. Pei, B.-J. Zhong, S. Som, T. Lu, K. H. Luo, A compact skeletal mechanism for n-dodecane with optimized semi-global low-temperature chemistry for diesel engine simulations, Fuel 191 (2017) 339–349.

[15] M. S. Day, J. B. Bell, Numerical simulation of laminar reacting flows with complex chemistry, Combustion Theory and Modelling 4 (2000) 535–556.

[16] D.-H. Shin, E. S. Richardson, V. Aparece-Scutariu, Y. Minamoto, J. H. Chen, Fluid age-based analysis of a lifted turbulent dme jet flame dns, Proceedings of the Combustion Institute 37 (2019) 2215 – 2222.